JOURNAL OF GEOPHYSICAL RESEARCH, VOL. 115, A06306, doi:10.1029/2009JA014984, 2010

Variabilities of the equatorial electrojet in Brazil and Perú

E. B. Shume,[1] C. M. Denardini,[1] E. R. de Paula,[1] and N. B. Trivedi[2]

Received 12 October 2009; revised 20 April 2010; accepted 3 May 2010; published 16 June 2010.

[1] This report presents seasonal and longitudinal variabilities of the equatorial electrojet in the east (Brazil, São Luís: 2.3° S; 315.8° E; 0.5° S dip latitude) and west (Jicamarca, Perú: 11.95° S; 283.13° E; 0.6° N dip latitude) coasts of the continent of South America. Ground-based magnetic field perturbation measurements ΔH for solar maximum (2001/2002) and solar minimum (2006/2007) conditions from the two equatorial stations (São Luís and Jicamarca) have been used for the study. The ΔH signal which is a measure of the strength of the equatorial electrojet is spectrally analyzed using wavelet analysis. The results of our analysis show that (1) the equatorial electrojet has maxima around equinoxes in Jicamarca, Perú but it has a prominent maximum during Southern Hemisphere summer (centered about December/January) in São Luís, Brazil. The observed seasonal behavior of the equatorial electrojet in São Luís is highly likely due to the large magnetic declination angle (about 20° west) there. (2) The equatorial electrojet is stronger in the west coast (Jicamarca) compared to the east coast (São Luís), irrespective of solar activity condition. (3) The magnitude of the equatorial electrojet is more variable with season and solar cycle over São Luís than over Jicamarca.

Citation: Shume, E. B., C. M. Denardini, E. R. de Paula, and N. B. Trivedi (2010), Variabilities of the equatorial electrojet in Brazil and Perú, *J. Geophys. Res.*, *115*, A06306, doi:10.1029/2009JA014984.

1. Introduction

[2] The equatorial electrojet is a strong electric current flowing in the *E* region of the equatorial ionosphere. The regular course of the current flow is eastward during daytime and westward at night. The equatorial electrojet can cause a net deflection of about 200 nT on ground magnetometers during solar maximum conditions. The physical mechanism for generating the equatorial electrojet is a complex interaction between: Horizontal geometry of the geomagnetic field in the proximity of the magnetic equator, anisotropy in ionospheric conductivities, the confinement of the Hall conductivity in a finite slab, the solar tide driven dynamo, and the resulting horizontal and vertical polarization electric fields [*Richmond*, 1973a; *Forbes*, 1981; *Kelley*, 2009].

[3] Over the last several decades, extensive experimental and theoretical research has been carried out to study the equatorial electrojet [*Sugiura and Poros*, 1969; *Richmond*, 1973a, 1973b; *Forbes*, 1981; *Onwumechili and Agu*, 1981; *Onwumechili*, 1997; *Chandra et al.*, 2000; *Hysell et al.*, 2002; *Lühr et al.*, 2004; *Rastogi et al.*, 2007, and the references therein]. Among these research endeavors, long-term ground- and space-based magnetic field measurements have been instrumental for studying the diurnal, seasonal, longitudinal, latitudinal, and solar cycle variabilities of the equatorial electrojet. We have here referred to some of the ground and in situ magnetic field observations which are relevant for the research at hand.

[4] 1. Ground-based [*Chandra et al.*, 2000; *Okeke and Hamano*, 2000; *Doumouya et al.*, 2003; *Rastogi et al.*, 2007] and satellite-based [*Onwumechili and Agu*, 1981; *Jadhav et al.*, 2002; *Alken and Maus*, 2007] horizontal magnetic field measurements have indicated that the equatorial electrojet has diurnal periodicity with maximum around local noon.

[5] 2. The magnitude of the equatorial electrojet is generally higher during solar maximum conditions compared to solar minimum conditions [*Forbes*, 1981; *Chandra et al.*, 2000; *Le Mouel et al.*, 2006].

[6] 3. The equatorial electrojet in the Pacific, African, and Indian longitude sectors [*Chapman and Rao*, 1965] have equinoctial maximum and solstitial minimum (based on ground-based magnetometer data). Similar conclusions have been drawn utilizing networks of ground-based magnetic field observations in the Indian [*Rastogi et al.*, 1994], West African [*Doumouya et al.*, 1998], and Japanese [*Okeke and Hamano*, 2000] longitude sectors. These seasonal variabilities have also been confirmed by magnetic field measurements on board CHAMP satellite [*Le Mouel et al.*, 2006; *Alken and Maus*, 2007].

[7] 4. The magnitude of the equatorial electrojet varies longitudinally, according to POGO [*Onwumechili and Agu*, 1981, 1982; *Kim and King*, 1999], Ørsted [*Jadhav et al.*, 2002; *Ivers et al.*, 2003; *Alken and Maus*, 2007] and CHAMP [*Lühr et al.*, 2004; *Le Mouel et al.*, 2006; *Alken*

[1]Aeronomy Division, National Institute for Space Research, São Paulo, Brazil.
[2]Space Geophysics Division, National Institute for Space Research, São Paulo, Brazil.

0148-0227/10/2009JA014984

and Maus, 2007] satellite magnetic field measurements. Ground-based magnetic field measurements have also shown that the magnitude of equatorial electrojet is stronger in the Pacific sector at Huancayo (Perú) than in the Atlantic sector at Fortaleza (Brazil) [*Kane and Trivedi*, 1982] and in the Indian equatorial longitude sector [*Rastogi*, 1962; *Doumouya et al.*, 2003]. The electrojet is also stronger in the Pacific sector at Ancon (Perú) than the Atlantic sector in São Luís (Brazil) [*Rastogi et al.*, 2007].

[8] In the present study, we investigate the seasonal and longitudinal variability of the equatorial electrojet on the east coast (São Luís, Brazil: 2.3° S; 315.8° E; 0.5° S dip latitude) and west coast (Jicamarca, Perú: 11.95° S; 283.13° E; 0.6° N dip latitude) of the continent of South America. To carry out these objectives, we have used a wavelet analysis technique to spectrally analyze the hourly averaged horizontal magnetic field perturbation ΔH (which is a measure of the strength of the equatorial electrojet) time series for a year at solar maximum (2001/2002) and solar minimum (2006/2007) conditions from the two equatorial magnetometer stations on the east and west coasts of South America, São Luís and Jicamarca, respectively. The fact that the magnetic declination angle in São Luís (which is about −20.3°) is much larger than in Jicamarca (which is about −0.3°) is an impetus to make a comparative variability study in these two longitude sectors. Consequently, our study addresses the following specific questions.

[9] 1. How does the strength of the equatorial electrojet current vary seasonally in the east (São Luís, Brazil) and west (Jicamarca, Perú) coasts of South America? How do the seasonal and solar cycle variabilities compare between the east and west coasts of South America?

[10] 2. How does the equatorial electrojet vary longitudinally between the east coast (Brazil) and west (Perú) coast of South America for different seasons and solar activity conditions?

[11] This manuscript is organized according to the following order: section 2 describes the method of estimating ground-based horizontal magnetic field perturbation measurements ΔH (signature of the equatorial electrojet), and the method of spectrally analyzing the resulting ΔH time series using the wavelet analysis technique. Wavelet power spectra showing seasonal, solar cycle, and longitudinal variabilities of the equatorial electrojet on the east coast (São Luís, Brazil) and west coast (Jicamarca, Perú) longitude sectors of South America are presented and discussed in section 3. Summary and conclusions are given in section 4.

2. Data Presentation and Analysis Technique

2.1. Ground-Based Magnetic Field Measurements

[12] The strength of the equatorial electrojet is commonly measured by ground-based magnetometers located at equatorial stations. Estimating ΔH, which is a measure of the strength of the equatorial electrojet, involves the following procedures. (1) Nighttime baseline magnetometer records for the four stations used in our study (Jicamarca, Perú, Piura, Perú, São Luís, Brazil, and Eusébio, Brazil) are subtracted out to obtain daytime values at each station. The baseline record is an average of midnight values of five geomagnetically quiet days. This baseline value was first subtracted out to get daytime magnetic field values. (2) The daytime values (residuals after the baseline removal) are then used to calculate ΔH. ΔH is obtained by calculating the difference in magnitude of the measured horizontal magnetic field component between a magnetometer placed on the magnetic equator and one placed 6 to 9 degrees away (a magnetometer placed outside the influence of the equatorial electrojet). These procedures have also been implemented by *Rastogi and Klobuchar* [1990] and *Anderson et al.* [2002, 2004, 2006]. Accordingly, horizontal magnetic field residues ΔH at Jicamarca, Perú, (11.95° S; 283.13° E; 0.6° N dip latitude) are obtained by subtracting from them magnetic field measurements at Piura, Perú (5.11° S; 279.66° E; 6.67° N dip latitude). We have used similar procedures to determine ΔH at São Luís, Brazil (2.3° S; 315.8° E; 0.5° S dip latitude) using off-dip-equator data from a magnetometer placed at Eusébio, Brazil (3.8° S; 321.6°; 6.3° S dip latitude). The resulting ΔH time series for solar maximum (2001/2002) and solar minimum (2006/2007) conditions for the two equatorial stations, Jicamarca and São Luís, are displayed in Figures 1a, 2a, 3a, and 4a, respectively. The ΔH signal is spectrally analyzed using a wavelet analysis technique as described below.

2.2. Data Analysis Technique

[13] We have applied the wavelet analysis technique [*Kumar and Foufoula-Georgiou*, 1997; *Torrence and Compo*, 1998] to the ΔH time series to identify the dominant (periodicity) seasonality and longitudinal variations. We have employed the Mexican hat wavelet (equation (2)) for our analysis here because of its close resemblance with the shape of the equatorial electrojet current.

[14] The wavelet transform (equation (1)) can be defined as a convolution of a family of wavelet functions $\Psi_{a,b}(t)$ with the $\Delta H(t)$ signal:

$$\mathcal{H}(a,b) = \int_{-\infty}^{\infty} \Delta H(t) \Psi_{a,b}(t) dt \tag{1}$$

where t stands for time, a is a scale (dilation and contraction) factor, b is a translation factor, and the Mexican hat wavelet is defined in equation (2) using $\eta \equiv \frac{t-b}{a}$ (the function $\Psi(t)$ below is the Mother Mexican hat wavelet)

$$\Psi_{a,b}(t) = \frac{1}{\sqrt{a}} \Psi(\eta) = \frac{1}{\sqrt{a}} \frac{2}{\sqrt{3}} \pi^{-1/4} (1-\eta^2) \exp(-\eta^2/2), \quad a > 0 \tag{2}$$

[15] In our spectral calculation we used, $a_j = a_\circ 2^{j*\delta j}$ hours, where $j = 1, 2, \ldots, 96$, $a_\circ = 2\delta t = 2$, the time spacing $\delta t = 1$, and $\delta j = 0.125$ for adequate sampling in the scale [*Torrence and Compo*, 1998]. The translation factor $b_j = j$ hours, where $j = 0, 1, 2, 3, \ldots$ until end of the time series. The scale a is related to the vertical axis (or period) in Figures 1b, 2b, 3b, and 4b (period = $\frac{2\pi a}{\sqrt{2.5}}$, for Mexican hat wavelet) [*Torrence and Compo*, 1998]. The parameter b translates the wavelet function through the time series for a given value of the scale parameter a.

[16] We seek for dominant spectral features in the ΔH time series, by convolution of the Mexican hat wavelet (equation (2)) with the ΔH time series as shown in equation (1). The resulting wavelet power spectra $|\mathcal{H}(a, b)|^2$

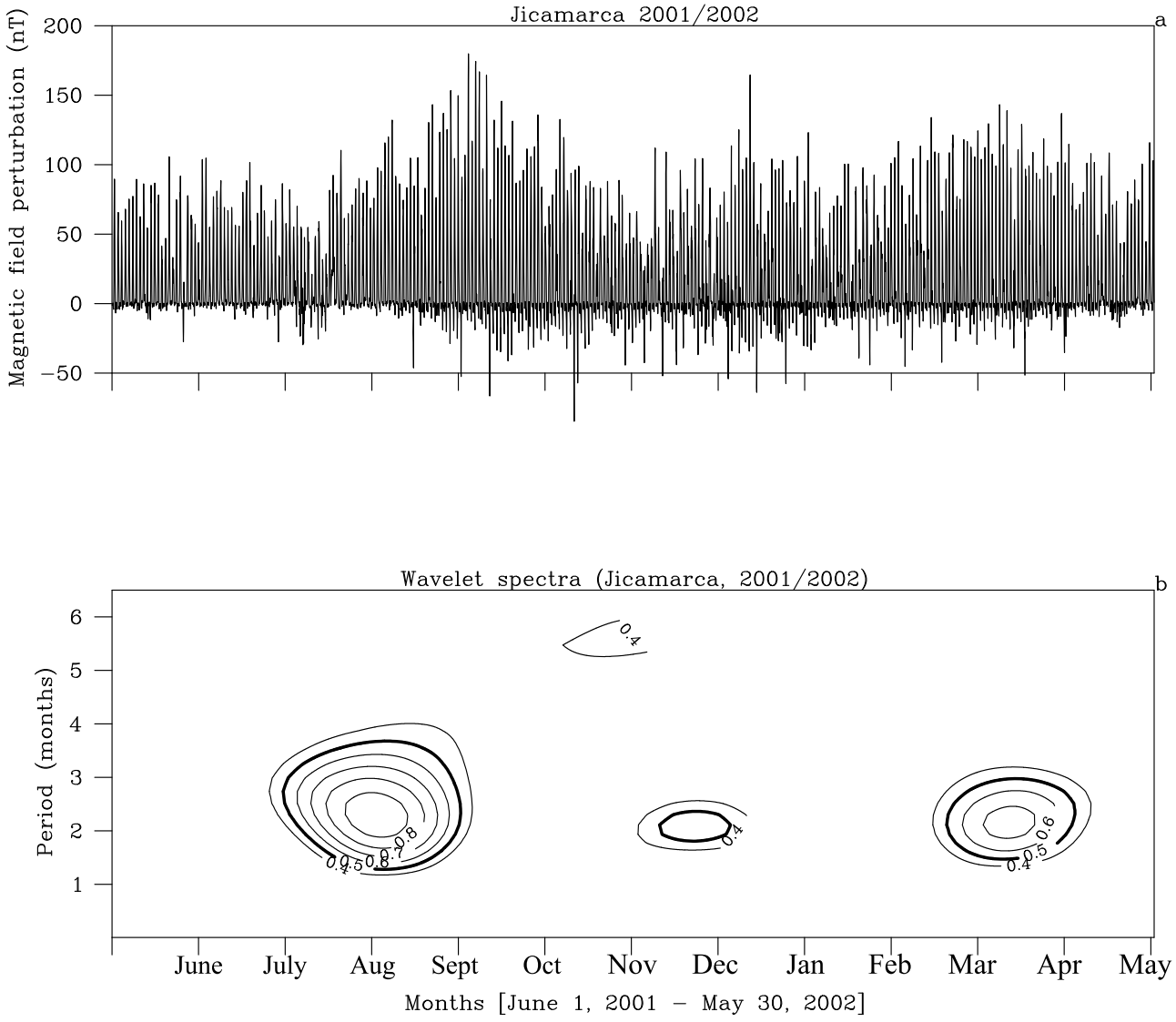

Figure 1. (a) Time series of measured horizontal magnetic field perturbations ΔH in the Peruvian sector in Jicamarca for solar maximum conditions 2001/2002. (b) Wavelet power spectra (nT^2 hour) of the magnetic field perturbation ΔH signal in Jicamarca for 2001/2002.

for solar maximum and minimum conditions in Jicamarca, Perú and São Luís, Brazil are shown in Figures 1b, 2b, 3b, and 4b, respectively. Scale-averaged normalized wavelet power spectra for São Luís and Jicamarca are shown in Figure 5. The maximum value of the four power spectra (Jicamarca 2001/02, Jicamarca 2006/07, São Luís 2001/02, and São Luís 2006/07) was used to normalize the individual power spectrum shown in Figure 5. Section 3 discusses the significance of these wavelet power spectra to understand the seasonal and longitudinal variations of the equatorial electrojet in Jicamarca and São Luís.

3. Results and Discussion

3.1. Wavelet Power Spectra

[17] Time series of the ground-based magnetic field perturbation ΔH measured in Jicamarca, Perú for solar maximum (2001/2002) and solar minimum (2006/2007) conditions are shown in Figures 1a and 2a, respectively. Wavelet power spectra $|\mathcal{H}(a, b)|^2$ for the ΔH signals in Figures 1a and 2a are shown in Figures 1b and 2b, respectively. The contour curves in Figures 1b and 2b demonstrate that the normalized wavelet power has maximum around August/September and April, and minimum around June and November/January suggesting generally equinoctial maximum and solstitial minimum of the equatorial electrojet in Jicamarca, Perú. The results shown by the wavelet power spectra are in agreement with the findings of *Chapman and Rao* [1965], *Rastogi et al.* [1994], *Doumouya et al.* [1998], and *Okeke and Hamano* [2000]. For solar maximum years 2001/2002, the two prominent peaks of the power spectrum have periods of about 2 months. For solar minimum years 2006/2007, the spectral power peaks have periods of about $1\frac{1}{2}$ (around August/September) and a little more than 1 month (around April). These periods are approximately equal to the length of the respective equinox

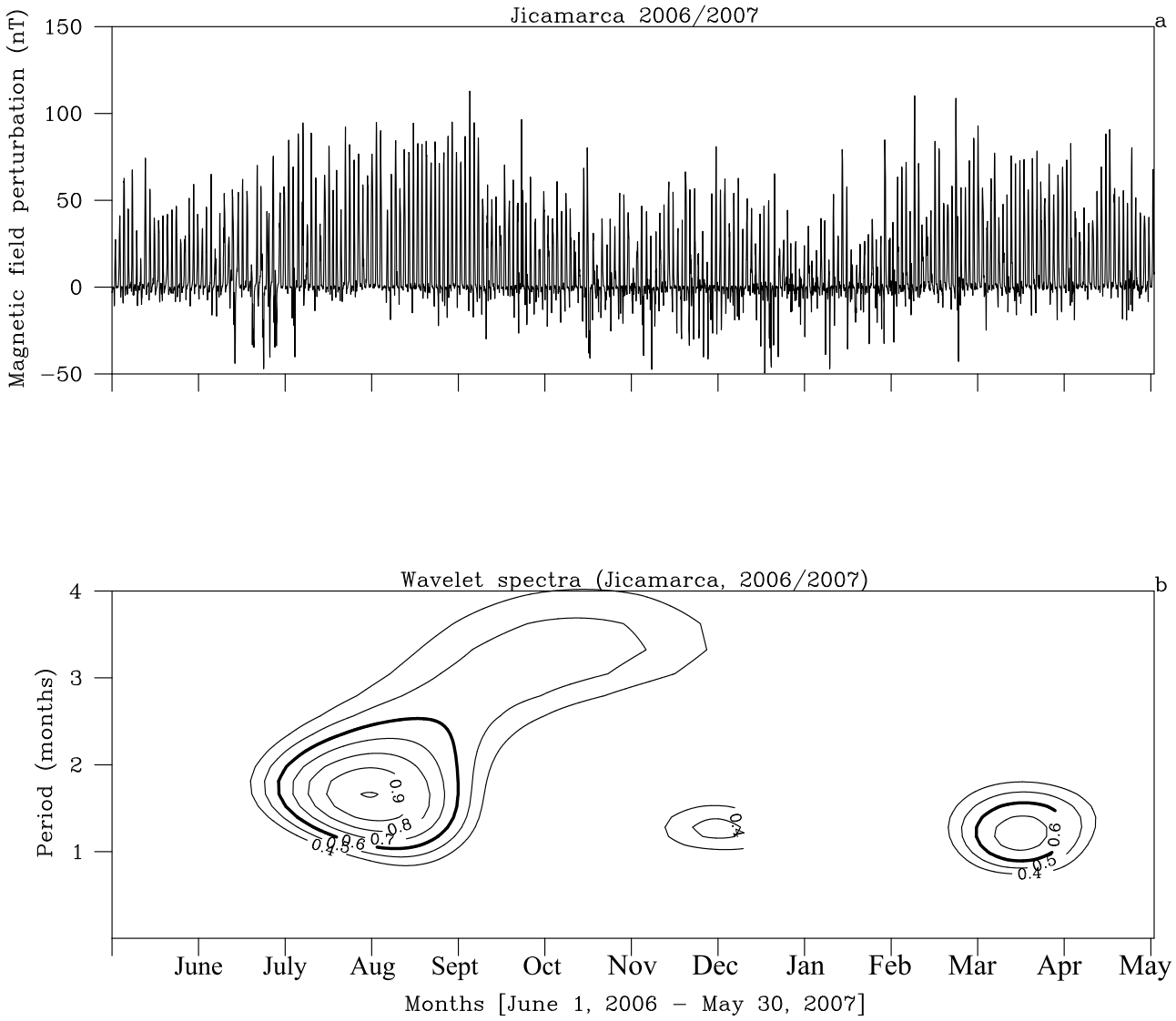

Figure 2. (a) Same as Figure 1a but for solar minimum conditions 2006/2007 in Jicamarca. (b) Same as Figure 1b but for solar minimum conditions 2006/2007 in Jicamarca.

seasons (which can be about 1 to 2 months). Different normalizations were used for the solar maximum (Figure 1b) and solar minimum (Figure 2b) wavelet power spectra. The thick contour lines in Figures 1b and 2b enclose regions of 95% confidence level of the wavelet power spectra. The assumption made in the calculation of the confidence level is that if a peak in the wavelet power spectrum is significantly above a background (red or white noise) spectrum, then it can be assumed to be a true feature with a certain percent confidence [*Torrence and Compo*, 1998].

[18] Time series of ΔH measured in São Luís, Brazil for solar maximum (2001/2002) and solar minimum (2006/2007) conditions are shown in Figures 3a and 4a, respectively. Wavelet power spectra of the ΔH signals are shown in Figures 3b and 4b. Contrary to the power spectra for Jicamarca, in Figures 3b and 4b, the normalized wavelet power (shown by the contour curves) is concentrated around December/January. This indicates that the equatorial electrojet in São Luís, Brazil is characterized by solstitial maximum (centering around December/January). In Figures 3b and 4b, the power spectra are characterized by one peak centering around December/January with a period of a little less than 6 months (2001/2002) and 5 months (2006/2007). These periods are again approximately equal to the length of the respective solstitial seasons in São Luís (which can be about 5 to 6 months). Using monthly averaged magnetic field data for five international quiet days, *Rastogi et al.* [2007] have concluded that the equatorial electrojet in São Luís, Brazil has equinoctial maxima (March) and solstitial minima (June). The magnetic field data used for our investigation is long term and has greater time resolution (hourly averaged ΔH data in 2001/2002 and 2006/2007 with few dropouts), we therefore believe that the seasonal behavior of the equatorial electrojet is captured very well by the present study. Our analysis shows also that despite the fact that São Luís and Jicamarca are only separated by about 30° of longitude, the equatorial electrojet has distinct seasonal and longitudinal characteristics in the two longitude

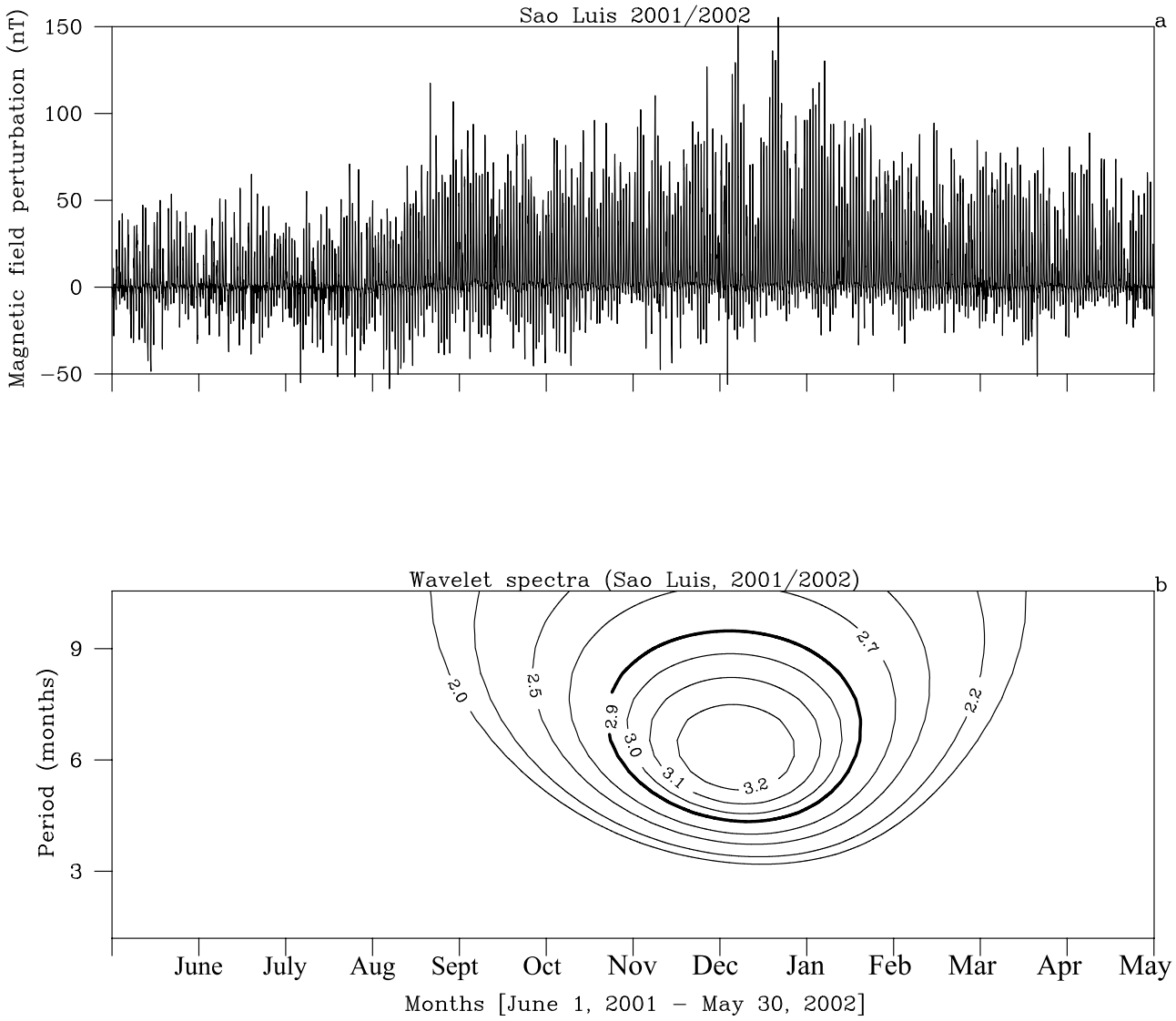

Figure 3. (a) Time series of measured horizontal magnetic field perturbations ΔH in the Brazilian sector in São Luís for solar maximum condition 2001/2002. (b) Wavelet power spectra (nT^2 hour) of the ΔH signal in São Luís for 2001/2002.

sectors. In this case too, different normalizations were used for the solar maximum (Figure 3b) and solar minimum (Figure 4b) wavelet power spectra. The 95% confidence level of the wavelet power spectra are also enclosed by thick solid lines in Figures 3b and 4b.

[19] In order to learn more about the seasonal and longitudinal variabilities of the magnetic field data ΔH, we have performed scale averaging (average of the wavelet power spectra over scales a_j) of the wavelet power spectra. The wavelet power spectra shown in Figures 1b, 2b, 3b, and 4b were averaged around the periods where the maximum power is concentrated. The average normalized wavelet power in Jicamarca and São Luís for solar maximum (2001/2002) and minimum (2006/2007) conditions are shown in Figures 5a–5d (in this case, the wavelet power spectra were normalized using the same normalization). Figures 5a–5d show that irrespective of solar activity condition, the equatorial electrojet has a larger magnitude in Jicamarca than São Luís suggesting longitudinal inhomogeneity of strength of the electrojet between the east and west coasts of South America. The longitudinal variation of the electrojet in these two sectors has also been reported by *Rastogi et al.* [2007]. Observing Figures 5b and 5c, it might also be worth mentioning that average wavelet power at Jicamarca during solar minimum (2006/2007) is only a little less than or comparable to that of average power of São Luís during solar maximum (2001/2002). As mentioned earlier each individual spectra were normalized using the same normalization factor. Average wavelet power shown in Figures 5a and 5b (Jicamarca) are out of phase with average power in Figures 5c and 5d (São Luís) indicating the unique seasonal characteristics of the equatorial electrojet on the east and west coasts of South America which is highly likely to be caused by the difference in the magnetic declination angle in the two longitude sectors. Comparison of scale-averaged wavelet spectra in Figure 5 also shows that the magnitude of the

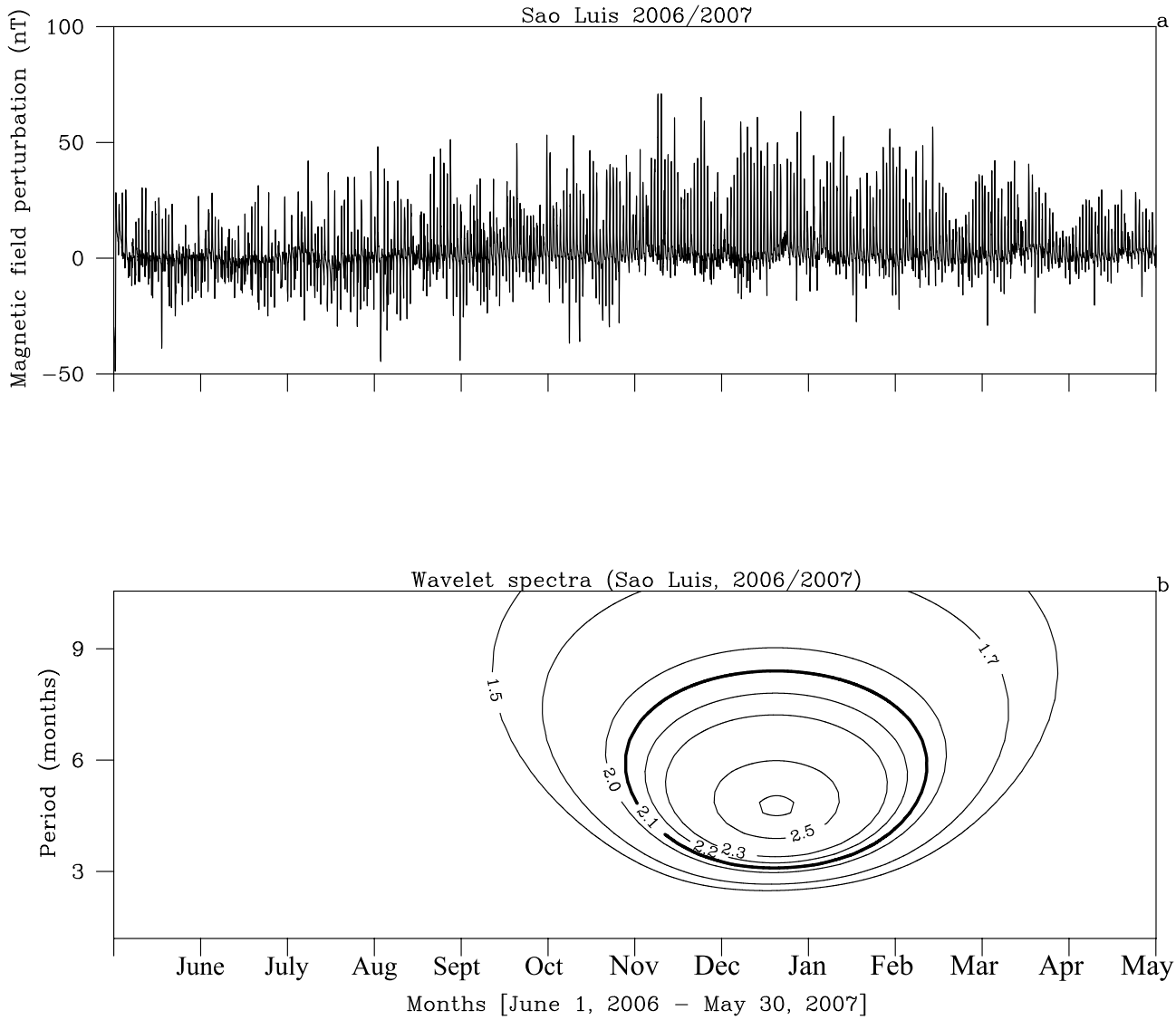

Figure 4. (a) Same as Figure 3a but for solar minimum condition 2006/2007 in São Luís. (b) Same as Figure 3b but for solar minimum condition 2006/2007 in São Luís.

equatorial electrojet is highly variable with season and solar cycle in São Luís compared to Jicamarca. Using incoherent scatter radar drift measurements from the Jicamarca Observatory *Fejer and Scherliess* [2001] studied the variability of equatorial *F* region vertical plasma drifts. They have shown that the daytime average upward drifts do not vary much with solar activity, but the evening upward and the nighttime downward drifts increase from solar minimum to solar maximum. Their data also indicated that the quiet time variability of the Jicamarca vertical drifts is local time, seasonal, and solar cycle dependent.

3.2. Seasonal Variations

[20] Due to difference in the magnetic declination angle on the east and west coasts of South America, the strength of the evening *F* region zonal electric field enhancement [*Abdu et al.*, 1981; *Batista et al.*, 1986] and frequency of occurrence of spread *F* plasma instabilities [*Abdu et al.*, 1981, 1992] have opposite seasonal characteristics in the two longitude sectors. Among the factors contributing to the difference in seasonal variability of the equatorial electrojet in São Luís and Jicamarca (depicted in the wavelet power spectra in Figures 1b, 2b, 3b, and 4b) might be, therefore, the difference in the magnetic declination angle in the two equatorial stations, which are about −20.3° and −0.3°, respectively. Given this geometry of the geomagnetic field, the seasonal variations in the wavelet power spectra (Figures 3b and 4b) and the strength of the equatorial electrojet in São Luís might be caused by a significant difference with season in the coupling between the equatorial *F* and the off-equatorial *E* regions. Equatorial *F* region winds influence the magnitude of the background zonal electric field and the equatorial electrojet (equivalently, magnetic field perturbation ΔH) [*Fang et al.*, 2008]: Westward winds in the equatorial *F* region generate an upward polarization electric field to counter divergence of the downward wind-driven Pedersen current. This electric field is mapped to the off-equatorial *E* region along the equipotential magnetic

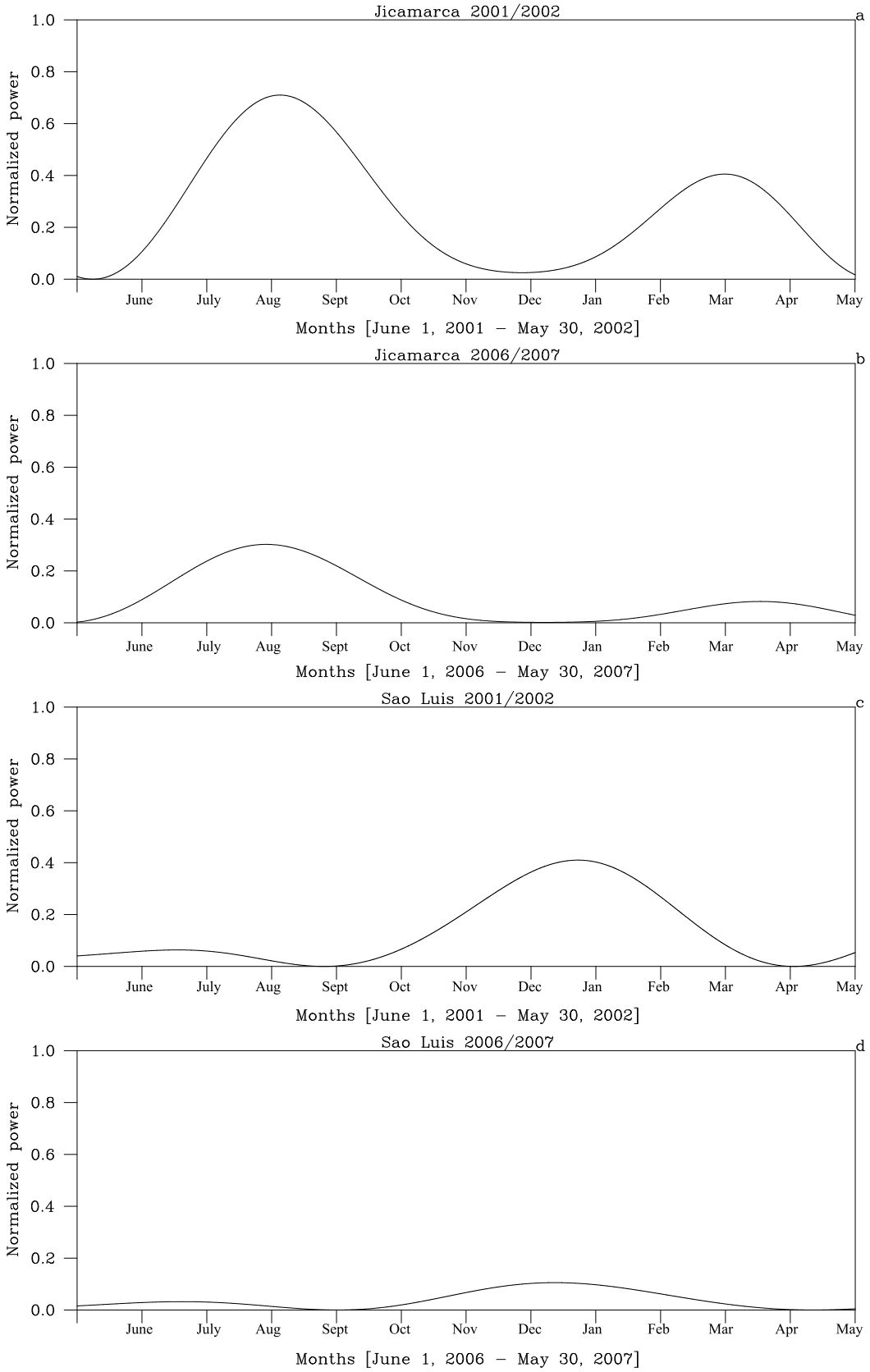

Figure 5. Scale-averaged wavelet power spectra for (a) solar maximum (2001/2002) condition in Jicamarca, Perú; (b) solar minimum (2006/2007) condition in Jicamarca; (c) solar maximum (2001/2002) condition in São Luís, Brazil; (d) solar minimum (2006/2007) condition in São Luís (same normalization has been used for the four cases).

field lines to drive an eastward Hall current there. An eastward Hall current decreases the background zonal electric field by decreasing polarization charge accumulation at the solar terminators. A decreased eastward electric field scenario contributes to a decrease in the strength of the electrojet ΔH. Electric field mapping from the F region to the E region (and influence of wind-driven electric field on the electrojet ΔH) is most likely efficient in São Luís (and east coast of South America) during equinoxes and June solstice months. During equinoxes and June solstice months, the large magnetic declination angle there is such that, the E and F ionospheric regions connected by the same magnetic meridian plane might not simultaneously maintain a high level of conductivity (the E region can be less conductive than the F region). During Southern Hemisphere summer (centered about the December/January), however, the highly conducting E region, which maintains a significant amount of conductivity for most of the day, might short-out polarization electric fields generated by the F region dynamo.

3.3. Longitudinal Variations

[21] As indicated above, ground-based magnetic field measurements have shown that the equatorial electrojet varies longitudinally within the South American continent between São Luís and Jicamarca. Evidence of satellite-based measurements of the equatorial electrojet showing longitudinal variations have also been reported [*Jadhav et al.*, 2002; *Ivers et al.*, 2003; *Lühr et al.*, 2004; *Le Mouel et al.*, 2006; *Alken and Maus*, 2007; *Lühr et al.*, 2008]. These in situ observations (specifically by *Jadhav et al.* [2002], *Ivers et al.* [2003], *Le Mouel et al.* [2006], and *Lühr et al.* [2008]) clearly show that the equatorial electrojet is stronger above the west coast (Perú) than the east coast (Brazil) of South America.

[22] The equatorial ionosphere is believed to be dynamically coupled with the neutral atmosphere through atmospheric tides propagating from the underlying atmosphere [*Sagawa et al.*, 2005; *England et al.*, 2006a; *Immel et al.*, 2006; *England et al.*, 2006b; *Hagan et al.*, 2007; *Kil et al.*, 2007; *Vineeth et al.*, 2007; *Forbes et al.*, 2008; *Lühr et al.*, 2008; *Immel et al.*, 2009]. The coupling between the ionosphere and the neutral atmosphere has been demonstrated in the quasi 16 day modulation of the equatorial electrojet by atmospheric tides [*Vineeth et al.*, 2007]. The coupling has also been revealed in the consistency of the longitudinal variations of the magnitude of the equatorial electrojet with the longitudinal variation in the strength of diurnal tides that drive the dynamo electric fields [*England et al.*, 2006b; *Kil et al.*, 2007]. The diurnal eastward propagating tidal mode with wave number-3 (DE3) has also been shown to have a dominant influence on the longitudinal structure of the equatorial electrojet [*Lühr et al.*, 2008]. Longitudinal variation of the strength of the equatorial electrojet between São Luís (Brazil) and Jicamarca (Perú) might be therefore caused by the difference in the modulation of the E region dynamo electric field by atmospheric tides between the two longitude sectors. In the equatorial electrojet region, the background eastward electric field produced by polarization charge accumulation at the dawn and dusk solar terminators is modulated by equatorial and off-equatorial atmospheric tides. The resultant polarization electric field in turn modulates the amplitude of the equatorial electrojet (or ΔH).

4. Summary and Conclusions

[23] This manuscript presents seasonal, solar cycle, and longitudinal variabilities of the equatorial electrojet above the east (São Luís, Brazil: 2.3° S; 315.8° E; 0.5° S dip latitude) and west (Jicamarca, Perú: 11.95° S; 283.13° E; 0.6° N dip latitude) coasts of the continent of South America. Ground-based magnetic field perturbation measurements ΔH for solar maximum (2001/2002) and solar minimum (2006/2007) conditions from the two equatorial stations (São Luís and Jicamarca) have been used for our study. The ΔH signal which is a measure of the strength of the equatorial electrojet is spectrally analyzed using wavelet analysis. The Mexican hat wavelet has been employed for our analysis here because of its close resemblance to the shape of the equatorial electrojet current. Dominant spectral features (seasonal and longitudinal variations) in the ΔH time series have been sought for by convolution of the Mother Mexican hat wavelet with the ΔH signal.

[24] The results of the wavelet spectral analysis have shown that (1) The equatorial electrojet varies longitudinally in South America. It is stronger on the west coast (Jicamarca) compared to the east coast (São Luís) of South America, irrespective of solar activity condition. (2) The equatorial electrojet has maximum strength during equinoxes (April and August/September) in Jicamarca, Perú but it has a prominent maximum in solstice season (centered about the month of December/January) in São Luís, Brazil. It is highly likely that seasonal variation of the electrojet in São Luís is controlled by the large magnetic declination angle (about 20° west) there. Given this geometry of the geomagnetic field, the likelihood of modulation of the equatorial electrojet by wind-driven dynamo electric field structures is high around equinoxes and June solstice seasons when the E and F ionospheric regions connected by the same magnetic field lines might not simultaneously maintain high level of conductivity (the E region can be less conducting than the F region). (3) The magnitude of the equatorial electrojet is highly variable with season and solar cycle on the east coast in São Luís compared to the west coast in Jicamarca.

[25] **Acknowledgments.** E. Shume is supported by FAPESP under project number 2007/08185-9 at INPE. C. M. Denardini thanks CNPq for the financial support (305923/2008-0). The Jicamarca Radio Observatory is a facility of the Instituto Geofsico del Perú operated with support from the NSF Cooperative Agreement ATM-0432565 through Cornell University. The authors thank I. S. Batista and M. A. Abdu for useful discussions.

[26] Robert Lysak thanks David Ivers and the other reviewers for their assistance in evaluating this paper.

References

Abdu, M. A., J. A. Bittencourt, and I. S. Batista (1981), Magnetic declination control of the equatorial F region dynamo electric field development and spread F, *J. Geophys. Res.*, *86*, 11,433–11,446.

Abdu, M. A., I. S. Batista, and J. H. A. Sobral (1992), A new aspect of magnetic declination control of equatorial spread F and F region dynamo, *J. Geophys. Res.*, *97*, 14,897–14,904.

Alken, P., and S. Maus (2007), Spatio-temporal characterization of the equatorial electrojet from CHAMP, Ørsted, and SAC-C satellite magnetic measurements, *J. Geophys. Res.*, *112*, A09305, doi:10.1029/2007JA012524.

Anderson, D., A. Anghel, K. Yumoto, M. Ishitsuka, and E. Kudeki (2002), Estimating daytime vertical **E** × **B** drift velocities in the equatorial F-region using ground-based magnetometer observations, *Geophys. Res. Lett.*, *29*(12), 1596, doi:10.1029/2001GL014562.

Anderson, D., A. Anghel, J. Chau, and O. Veliz (2004), Daytime vertical **E** × **B** drift velocities inferred from ground-based magnetometer observations at the low latitudes, *Space Weather*, *2*, S11001, doi:10.1029/2004SW000095.

Anderson, D., A. Anghel, J. L. Chau, and K. Yumoto (2006), Global, low-latitude, vertical **E** × **B** drift velocities inferred from daytime magnetometer observations, *Space Weather*, *4*, S08003, doi:10.1029/2005SW000193.

Batista, I. S., M. A. Abdu, and J. A. Bittencourt (1986), Equatorial F region vertical plasma drift: Seasonal and longitudinal asymmetries in the American sector, *J. Geophys. Res.*, *91*, 12,055–12,064.

Chandra, H., H. S. S. Sinha, and R. G. Rastogi (2000), Equatorial electrojet studies from rocket and ground measurements, *Earth Planets Space*, *52*, 111–120.

Chapman, S., and K. S. R. Rao (1965), The *H* and *Z* variations along and near the equatorial electrojet in India, Africa, and the Pacific, *J. Atmos. Terr. Phys.*, *27*, 559–581.

Doumouya, V., J. Vassel, Y. Cohen, O. Fambitakoye, and M. Menvielle (1998), Equatorial electrojet at African longitudes: First results from magnetic measurements, *Ann. Geophys.*, *16*, 658–676.

Doumouya, V., Y. Cohen, B. R. Arora, and K. Yumoto (2003), Local time and longitude dependence of the equatorial electrojet magnetic effects, *J. Atmos. Terr. Phys.*, *65*, 1265–1282.

England, S. L., T. J. Immel, E. Sagawa, S. B. Henderson, M. E. Hagan, S. B. Mende, H. U. Frey, C. M. Swenson, and L. J. Paxton (2006a), Effect of atmospheric tides on the morphology of the quiet time, post sunset equatorial ionospheric anomaly, *J. Geophys. Res.*, *111*, A10S19, doi:10.1029/2006JA011795.

England, S. L., S. Maus, T. J. Immel, and S. B. Mende (2006b), Longitudinal variation of the E-region electric fields caused by atmospheric tides, *Geophys. Res. Lett.*, *33*, L21105, doi:10.1029/2006GL027465.

Fang, T. W., A. D. Richmond, J. Y. Liu, and A. Maute (2008), Wind dynamo effects on ground magnetic perturbations and vertical drifts, *J. Geophys. Res.*, *113*, A11313, doi:10.1029/2008JA013513.

Fejer, B. G., and L. Scherliess (2001), On the variability of equatorial *F* region vertical plasma drifts, *J. Atmos. Sol. Terr. Phys.*, *63*, 893–897.

Forbes, J. M. (1981), The equatorial electrojet, *Rev. Geophys.*, *19*, 469–504.

Forbes, J. M., X. Zhang, S. Palo, J. Russell, C. J. Mertens, and M. Mlynczak (2008), Tidal variability in the ionospheric dynamo region, *J. Geophys. Res.*, *113*, A02310, doi:10.1029/2007JA012737.

Hagan, M. E., A. Maute, R. G. Roble, A. D. Richmond, T. J. Immel, and S. L. England (2007), Connections between deep tropical clouds and the Earth's ionosphere, *Geophys. Res. Lett.*, *34*, L20109, doi:10.1029/2007GL030142.

Hysell, D. L., J. L. Chau, and C. G. Fesen (2002), Effect of large scale horizontal winds on the equatorial electrojet, *J. Geophys. Res.*, *107*(A8), 1214, doi:10.1029/2001JA000217.

Immel, T. J., E. Sagawa, S. L. England, S. B. Henderson, M. E. Hagan, S. B. Mende, H. U. Frey, C. M. Swenson, and L. J. Paxton (2006), Control of equatorial ionospheric morphology by atmospheric tides, *Geophys. Res. Lett.*, *33*, L15108, doi:10.1029/2006GL026161.

Immel, T. J., S. B. Mende, M. E. Hagan, P. M. Kintner, and S. L. England (2009), Evidence of tropospheric effects on the ionosphere, *EOS Trans. AGU*, *90*(9), doi:10.1029/2009EO090001.

Ivers, D., R. Stening, J. Turner, and D. Winch (2003), Equatorial electrojet from Ørsted scalar magnetic field observations, *J. Geophys. Res.*, *108*(A2), 1061, doi:10.1029/2002JA009310.

Jadhav, G., M. Rajaram, and R. Rajaram (2002), A detailed study of equatorial electrojet phenomena using Ørtsed satellite observations, *J. Geophys. Res.*, *107*(A8), 1175, doi:10.1029/2001JA000183.

Kane, R. P., and N. B. Trivedi (1982), Comparison of equatorial electrojet characteristics at Huancayo and Eusébio (Fortaleza) in the South American region, *J. Atmos. Terr. Phys.*, *44*, 785–792.

Kelley, M. C. (2009), *The Earth's Ionosphere: Plasma Physics and Electrodynamics*, *Int. Geophys. Ser.*, vol. 96, Academic, San Diego, Calif.

Kil, H., S.-J. Oh, M. C. Kelley, L. J. Paxton, S. L. England, E. Talaat, K.-W. Min, and S.-Y. Su (2007), Longitudinal structure of the vertical E × B drift and ion density seen from ROCSAT-1, *Geophys. Res. Lett.*, *34*, L14110, doi:10.1029/2007GL030018.

Kim, H. R., and S. D. King (1999), A study of local time and longitudinal variability of the amplitude of the equatorial electrojet observed in POGO satellite data, *Earth Planets Space*, *51*, 373–381.

Kumar, P., and E. Foufoula-Georgiou (1997), Wavelet analysis for geophysical applications, *Rev. Geophys.*, *35*, 385–412.

Le Mouel, J.-L., P. Shebalin, and A. Chulliat (2006), The field of the equatorial electrojet from CHAMP data, *Ann. Geophys.*, *24*, 515–527.

Lühr, H., S. Maus, and M. Rother (2004), Noon-time equatorial electrojet: Its spatial features as determined by the CHAMP satellite, *J. Geophys. Res.*, *109*, A01306, doi:10.1029/2002JA009656.

Lühr, H., M. Rother, K. Häusler, P. Alken, and S. Maus (2008), The influence of nonmigrating tides on the longitudinal variation of the equatorial electrojet, *J. Geophys. Res.*, *113*, A08313, doi:10.1029/2008JA013064.

Okeke, F. N., and Y. Hamano (2000), Daily variations of geomagnetic *H*, *D*, and *Z*-field at equatorial latitudes, *Earth Planets Space*, *52*, 237–243.

Onwumechili, C. A. (1997), *The equatorial electrojet*, Gordon Breach, Newark, N. J.

Onwumechili, C. A., and C. E. Agu (1981), Longitudinal variation of equatorial electrojet parameters derived from POGO satellite observations, *Planet. Space Sci.*, *29*(6), 627–634.

Onwumechili, C. A., and C. E. Agu (1982), Regional variations equatorial electrojet parameters, *Ann. Geophys.*, *38*, 307–313.

Rastogi, R. G. (1962), Longitudinal variation in the equatorial electrojet, *J. Atmos. Terr. Phys.*, *24*, 1031–1040.

Rastogi, R. G., and J. A. Klobuchar (1990), Ionospheric electron content within the equatorial F_2 layer anomaly belt, *J. Geophys. Res.*, *95*, 19,045–19,052.

Rastogi, R. G., S. Alex, and A. Patil (1994), Seasonal variations of geomagnetic D, H, and Z at low latitudes, *J. Geomagn. Geoelectr.*, *46*, 115–126.

Rastogi, R. G., H. Chandra, D. Chakrabarty, K. Kitamura, and K. Yumoto (2007), Day-to-day correlation of equatorial electrojet at two stations separated by 2000 km, *Ann. Geophys*, *25*, 875–880.

Richmond, A. D. (1973a), Equatorial electrojet—I. Development of a model including winds and instabilities, *J. Atmos. Terr. Phys.*, *35*, *6*, 1083–1103.

Richmond, A. D. (1973b), Equatorial electrojet—II. Use of the model to study the equatorial ionosphere, *J. Atmos. Terr. Phys.*, *35*, *6*, 1105–11118.

Sagawa, E., T. J. Immel, H. U. Frey, and S. B. Mende (2005), Longitudinal structure of the equatorial anomaly in the nighttime ionosphere observed by IMAGE/FUV, *J. Geophys. Res.*, *110*, A11302, doi:10.1029/2004JA010848.

Sugiura, M., and D. J. Poros (1969), An improved model equatorial electrojet with a meridional current system, *J. Geophys. Res.*, *74*, 4025–4035.

Torrence, C., and G. P. Compo (1998), A practical guide to wavelet analysis, *Bull. Am. Meteorol. Soc.*, *79*, 61–78.

Vineeth, C., T. K. Pant, C. V. Devasia, and R. Sridharan (2007), Atmosphere-Ionosphere coupling observed over the dip equatorial MLTI region through the quasi 16-day wave, *Geophys. Res. Lett.*, *34*, L12102, doi:10.1029/2007GL030010.

C. M. Denardini, E. R. de Paula, and E. B. Shume, Aeronomy Division, National Institute for Space Research, INPE-DAE, Av. dos Astronautas, 1758, Jardim da Granja, 12227-010, São José dos Campos, São Paulo, Brazil. (esayas@dae.inpe.br)

N. B. Trivedi, Space Geophysics Division, National Institute for Space Research, INPE-DAE, Av. dos Astronautas, 1758, Jardim da Granja, 12227-010, São José dos Campos, São Paulo, Brazil.